Available online at www.sciencedirect.com
ScienceDirect
Polymer 48 (2007) 3504–3511
polymer
www.elsevier.com/locate/polymer

Direct analysis of annealing of nodular crystals in isotactic polypropylene by atomic force microscopy, and its correlation with calorimetric data

Qamer Zia, Hans-Joachim Radusch, René Androsch*

Martin-Luther-University Halle-Wittenberg, Center of Engineering Sciences, D-06099 Halle/Saale, Germany

Received 4 March 2007; received in revised form 6 April 2007; accepted 10 April 2007
Available online 19 April 2007

Abstract

The process of isothermal annealing of nodular monoclinic crystals of isotactic polypropylene (iPP) was analyzed by atomic force microscopy (AFM) and temperature-modulated differential scanning calorimetry (TMDSC). Initially nodular and mesomorphic domains were obtained by controlled melt-crystallization at high cooling rate. Subsequent heating triggers transition from mesomorphic to monoclinic structure, and melting of unstable nodules. Annealing allows re-crystallization, which is recognized by enlargement of domains from initially about 20 nm to about 35 and 55 nm after annealing at 393 and 433 K, respectively. Furthermore, the re-crystallization process is connected with a slight change of the aspect ratio of crystals. The isothermal re-crystallization of the liquid is superimposed by aggregation of crystals, to yield blocky, and string-like objects. The direct analysis of structure on isothermal annealing by AFM is for the first time compared with the isothermal decrease of the apparent specific heat capacity, or change of enthalpy, monitored by TMDSC. The apparent specific heat capacity decreases during annealing with an identical non-linear time dependence as the directly observed growth of the crystal size. Analysis of the annealing processes at different temperatures yields proportionality between the increase of the crystal size and the reduction of the apparent specific heat capacity.

Keywords: Isotactic polypropylene; Annealing; Atomic force microscopy (AFM)

1. Introduction

The structure and morphology of crystals of isotactic polypropylene (iPP) can largely be controlled by the condition of primary melt-crystallization. Slow cooling yields in absence of special nucleating agents monoclinic α-crystals, and fast cooling results in the formation of mesomorphic domains. The transition from formation of monoclinic crystals to formation of mesomorphic domains on melt-crystallization occurs at a critical rate of cooling of about 10^1 K s^{-1}–10^2 K s^{-1}, as was concluded from early investigations using density measurements and X-ray analyses [1–4]. In a recent study, it was found, by systematic analysis of the crystal morphology as a function of the cooling rate on melt-crystallization, that mesomorphic crystals exclusively are of globular shape, and that monoclinic crystals are of lamellar geometry [5]. The size of nodules after rapid cooling apparently is independent on the exact condition of quenching since only minor systematic changes of the size were detected as function of the rate of cooling. The size of nodules after quenching at 10^2 K s^{-1} is about 20 nm at ambient temperature and is only slightly decreased by about 10% when increasing the cooling rate to 10^3 K s^{-1} [5]. Further increase of the rate of cooling to 2×10^3 K s^{-1} completely suppresses crystallization and yields a totally amorphous polymer as long as the temperature is kept below the glass transition temperature of about 240–250 K [6].

The mesomorphic nodular domains transform on heating to monoclinic crystals at a temperature of about 340 K [7,8]. The transition from the mesomorphic to the monoclinic phase is a solid–solid first order phase transition since it occurs without complete prior melting of the parent phase at a local scale within the existing domains, and since it is connected with a change of the specific volume of the crystal phase [5]. The density of the monoclinic phase is larger than the density of

* Corresponding author. Tel.: +49 3461 46 3762; fax: +49 3461 46 3891.
E-mail address: rene.androsch@iw.uni-halle.de (R. Androsch).

0032-3861/$ - see front matter © 2007 Elsevier Ltd. All rights reserved.
doi:10.1016/j.polymer.2007.04.012

the mesomorphic phase which is mainly achieved by adjustment of the handness of helices, resulting in a higher lateral packing density of molecules in the monoclinic structure [9]. The conclusion of only local readjustment of the handness of helices, and/or their repositioning within the ordered domains during the phase transition is derived from the unchanged morphology of crystals, i.e., the globular geometry and size of about 20 nm are preserved [5]. Further heating of the monoclinic nodular crystals to about 400 K is accompanied only by a small increase of the nodule dimension to about 25 nm. Major changes of the crystal morphology were observed if the temperature is raised to 400–430 K. In this temperature range, melting of smaller nodules occurs which finally allows, by removal of local strain within the semi-crystalline structure, drastic growth of still existing nodular crystals and their alignment for surface-energy reduction. The size of nodules increases to 60 nm, and the lateral alignment by coalescence yields curved, lamellae-like objects with visible internal surfaces [5].

The analysis of the temperature dependence of the geometry and dimension of crystals of iPP, generated on rapid, controlled melt-crystallization, is extended in the present study to evaluate the time dependence of the structural changes on annealing at elevated temperature. We focus on the temperature range above 390 K since at lower temperature, including the temperature range of the solid–solid phase transformation, reorganization with a change of the geometry of crystals is minor. Systematic studies on the effect of the annealing time on the reorganization of initially nodular and mesomorphic crystals were not performed yet. Former investigation of the shape and size of nodular crystals mainly included an evaluation of the effect of temperature, while the data were taken after a specified annealing time [9–13]. An early report which included an analysis of the time dependence on the morphology of initially nodular crystals suggests that there is only a minor effect of the time of isothermal annealing on the crystal shape and size [14]. In the particular study, the initial size of nodular crystals was 7.5–10 nm at ambient temperature. Annealing at 373 K for a period of 4 days yielded crystals of size of 10–20 nm without indication of an effect on annealing time. An additional annealing experiment at 411 K for periods of 2.5 h, 28 h and 4 days revealed a further increase of the crystal size to 20–30 nm, again being only slightly increasing as a function of time within the investigated interval from 2.5 h to 4 days. A complete analysis of the evolution of the crystal morphology as a function of time apparently is not available. Recent investigation of the isothermal annealing process of initially quenched iPP using temperature-modulated differential scanning calorimetry (TMDSC), however, suggests that reorganization follows an exponential law with the largest change of structure occurring at the early stage, within seconds or minutes [15,16]. Therefore we intend to monitor the crystal shape and size quasi-continuously as a function of time.

Annealing is synonymous for thermal treatment of a material for the sake of a controlled change of structure and, correspondingly, of properties. It includes as a special case the increase of the temperature to a pre-defined value, and keeping subsequently the temperature constant for a certain period of time. In general, the temperature of annealing is selected such that not all crystals are melted [17]. Within the isothermal segment of annealing of iPP, which is the focus of the present work, are expected processes like primary cold-crystallization, secondary crystallization, and crystal perfection, all of them controlled by the condition of prior melt-crystallization. Since melting is usually considered as a fast process [18], compared to crystallization, it is commonly assumed that melting of crystals of low stability occurs within the heating segment on approaching the final isothermal annealing temperature. All of these isothermally occurring processes are thermodynamically irreversible, i.e., these processes yield a new metastable global superstructure of reduced enthalpy. The decrease in the enthalpy is connected with a release of latent heat which can be measured by calorimetry. Since the amount of heat released during isothermal annealing is usually low, standard differential scanning calorimetry (DSC) often cannot be applied for direct monitoring of the annealing process, in particular if the reorganization of structure exceeds a large interval of time. In this case, the standard DSC signal, differential heat-flow rate as function of time, may be distorted by long-term non-reproducible instrumental drift. A convenient solution for elimination of instrumental disturbances is the application of temperature-modulated DSC (TMDSC) [19,20]. TMDSC allows a quasi-isothermal measurement of the apparent specific heat capacity [21], which contains a time-independent specific heat capacity contribution and a time-dependent latent-heat contribution [22]. Monitoring the time dependence of the apparent specific heat capacity can therefore provide detailed information about the kinetics of structural reorganization. Since the introduction of TMDSC, isothermal annealing experiments with simultaneous recording of the time dependence of the apparent specific heat capacity were performed on numerous semi-crystalline polymers including polyethylene [23–25], polypropylene [15,16], polyesters [26–28], and polytetrafluoroethylene [29]. During isothermal annealing, the apparent specific heat capacity decreases as a function of time to reach an equilibrium heat capacity. Unfortunately, the calorimetric signal cannot be assigned directly to specific changes of structure, i.e., interpretation of the isothermal decay of the apparent specific heat capacity is speculative if there are not performed additional, well-designed experiments which give direct structural information. Within the present study, an attempt is made to relate the calorimetrically measured reorganization process with direct observation of the time dependence of the crystal morphology.

Summarizing the scope of the present study, we intend to complete a recently performed study about the thermodynamic stability of initially mesomorphic and globular domains in iPP [5]. The temperature dependence on the nodule size and shape was analyzed in a preceding study as a function of the condition of the primary melt-crystallization, and within the present study we focus on the time dependence of the crystal morphology during isothermal annealing at elevated temperature, using atomic force microscopy (AFM). In the second part of this

study, we analyzed the kinetics of the isothermal annealing process by TMDSC, which allows for the first time a justified, structure-based interpretation of the decay of the apparent specific heat capacity.

2. Experimental

2.1. Materials

In the present study we used an iPP with a mass-average molar mass of 373 kg mol^{-1} and a polydispersity of 6.2, provided by Montell Polyolefins. The selected polymer is an extrusion-grade preparation for production of biaxially oriented films, with a melt-flow rate of 3.3 g/10 min, determined at 503 K with a load of 2.16 kg [30]. This polymer was investigated in detail in previous studies regarding the general thermal behavior, including reversible and irreversible crystallization and melting, annealing, and the crystal morphology [5,15,16].

Specimens with mesomorphic nodular crystals of initial size of about 20 nm were prepared with a special device for controlled rapid cooling, developed by Piccarolo [4]. In this study, we used samples which were crystallized at rates of cooling of 80 K s^{-1} and 750 K s^{-1}, effective at a temperature of 343 K. The thickness of films was 100 μm. The samples were solidified in contact with freshly cleaved mica, in order to obtain a sufficiently smooth surface for later AFM analysis. The annealing experiments were done on a Leitz hot-stage 1350, in combination with a Rheometric Scientific temperature controller. The hot stage was mounted on the sample stage of a polarizing microscope which allowed direct monitoring of the superstructure at the micrometer scale. The approach of the isothermal annealing temperature was done at a heating rate of 10 K min^{-1}. Subsequently, the samples were annealed for pre-defined periods of time up to 840 min. Then, the samples were cooled at 10 K min^{-1} to ambient temperature for morphological analysis by AFM. Each annealing experiment was done with a new sample.

2.2. Instrumentation

2.2.1. Microscopy

The crystal morphology was analyzed using a Quesant Q-Scope 250 AFM, equipped with a 40 μm × 40 μm scanner. We used standard silicon cantilevers NSC 16 with a resonant frequency and force constant of about 170 kHz and 40 N m^{-1}, respectively. Data were collected in tapping mode at ambient temperature.

2.2.2. Quantitative image analysis

The size of nodules was (a) computed using the AFM-image analysis software, and (b) additionally determined manually, by the line-intersection method on printouts. The total number of analyzed objects was about 50 and 100 per frame in computer aided and manual analysis of the size of nodules, respectively. In case of non-isotropic shape of nodules, the smaller dimension was considered for estimation of the size.

2.2.3. Temperature-modulated differential scanning calorimetry (TMDSC)

The isothermal annealing process was followed by TMDSC using a power-compensation-based differential scanning calorimeter DSC 7 from Perkin–Elmer. The instrument was operated in conjunction with the cryogenic cooling accessory CCA 7, ensuring a constant temperature of the heat sink of 223 K. The sample and reference furnaces were purged with nitrogen gas at a flow rate of 40 mL min^{-1}. Calibration of the sensor temperature and of the heat-flow rate was done according to standard procedures [31], using indium and tin as calibrants. Samples of mass of 1–2 mg were encapsulated in 20-μL aluminum pans from Mettler–Toledo, and heated to the annealing temperature at a rate of 10 K min^{-1}. Subsequent temperature modulation was done using a sawtooth-type temperature profile with a programmed amplitude and period of modulation of 1 K and 120 s, respectively [32,33]. Data were corrected for instrumental asymmetry by subtraction of a baseline, measured under identical condition as the sample. The baseline-corrected modulated heat-flow rate data were processed to an apparent specific heat capacity, using the instrument software. Finally, the apparent specific heat capacity was calibrated using sapphire as standard.

3. Results and initial discussion

3.1. Crystal morphology by AFM

Fig. 1 shows the structure of iPP, which was melt-crystallized on fast cooling at 80 K s^{-1} (left) and 750 K s^{-1} (right). The structure is heterogeneous and consists of nodular domains with an approximate size of 20 nm, embedded in an amorphous matrix. The X-ray data of a previous study suggest that the internal structure of the domains is mesomorphic [5]. The nodule size differs slightly, being smaller in the sample quenched at higher cooling rate. Manual quantitative analysis yields estimates of the nodule size of 21 and 18 nm for the samples cooled at 80 K s^{-1} and 750 K s^{-1}, respectively.

Figs. 2 and 3 show the evolution of the structures, which were shown in Fig. 1, as a function of time of isothermal annealing at 393 K (Fig. 2) and 433 K (Fig. 3). The top images were taken on the sample, which initially was crystallized at 80 K s^{-1}, and the bottom images were taken on the sample, which initially was crystallized at 750 K s^{-1}. The annealing time is 60, 440, 560, and 840 min, from left to right, being examples of larger sets of collected images. Further increase in the annealing time does not lead to additional changes of the structure in both cases, annealing at 393 and 433 K.

The images in Fig. 2 reveal an increase of the nodule size during isothermal annealing at 393 K. The geometry of the domain remains unchanged, i.e., the initial, nodular shape is preserved even after annealing for an extended period of time. The average crystal size changes from about 20 to almost 40 nm for both preparations.

Annealing at a temperature close to the final melting temperature results in the formation of considerably larger domains, as is documented by the images in Fig. 3. The

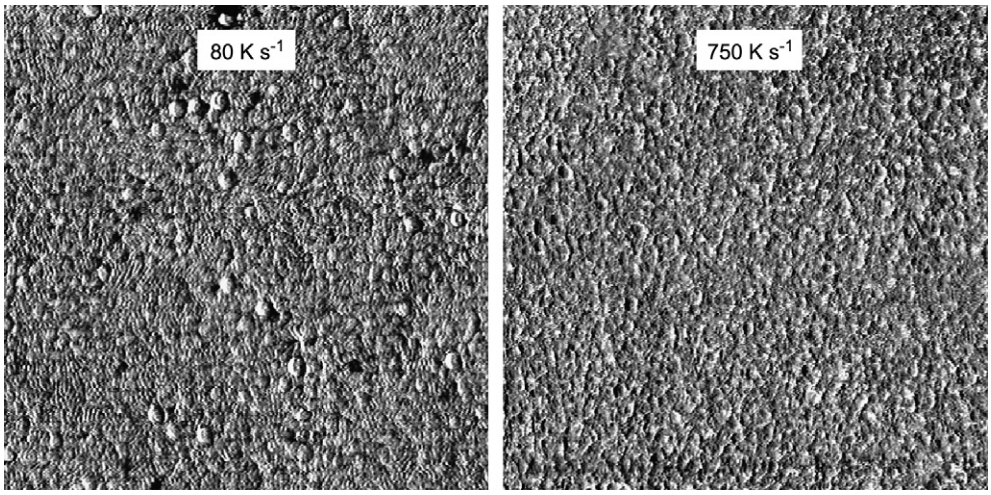

Fig. 1. AFM images of iPP, melt-crystallized at 80 K s^{-1} (left) and 750 K s^{-1} (right) cooling rate. The image size is 1 μm × 1 μm.

increase of the crystal size is three-fold since values close to 60 nm were detected, independent of the initial preparation. Furthermore we observed slight tendency for a change of the shape of crystals after annealing at 433 K. Initially, before annealing, the domains were isotropic in geometry. Annealing at 433 K yields crystals which are slightly larger in one of the two visible dimensions. This minor change of the crystal habit goes along with tendency for aggregation to form larger objects, which eventually can be considered as lamellae. The observation of a slight change of the aspect ratio of nodules and their aggregation is documented in Fig. 4, which is an enlargement of the bottom right image in Fig. 3. The above reported final size of nodules of almost 60 nm represents the smallest observed dimension of nodules which still can be analyzed after repositioning within aggregates.

Fig. 5 is a plot of the nodule size as function of the time of isothermal annealing. The open and filled symbols are data obtained on the samples which initially were melt-crystallized at 80 K s^{-1} and 750 K s^{-1}, respectively. The squares represent annealing at 433 K, and the diamonds represent annealing at 393 K. The lines were included to guide the eye, and are not a result of fitting or smoothing. The initial size of nodules is close to 20 nm. Heating to 393 K, and subsequent annealing increases the size of nodules to a final, quasi-equilibrium value of 36 nm. Annealing at 433 K yields a final value of the nodule size of 56 nm. In both cases, the approach of the final structure is non-linear, with only a minor, further increase of the nodule size by 1–2 nm after annealing for a period of about 500 min. Furthermore, we note that the condition of the initial primary melt-crystallization has no effect on the time-evolution of the

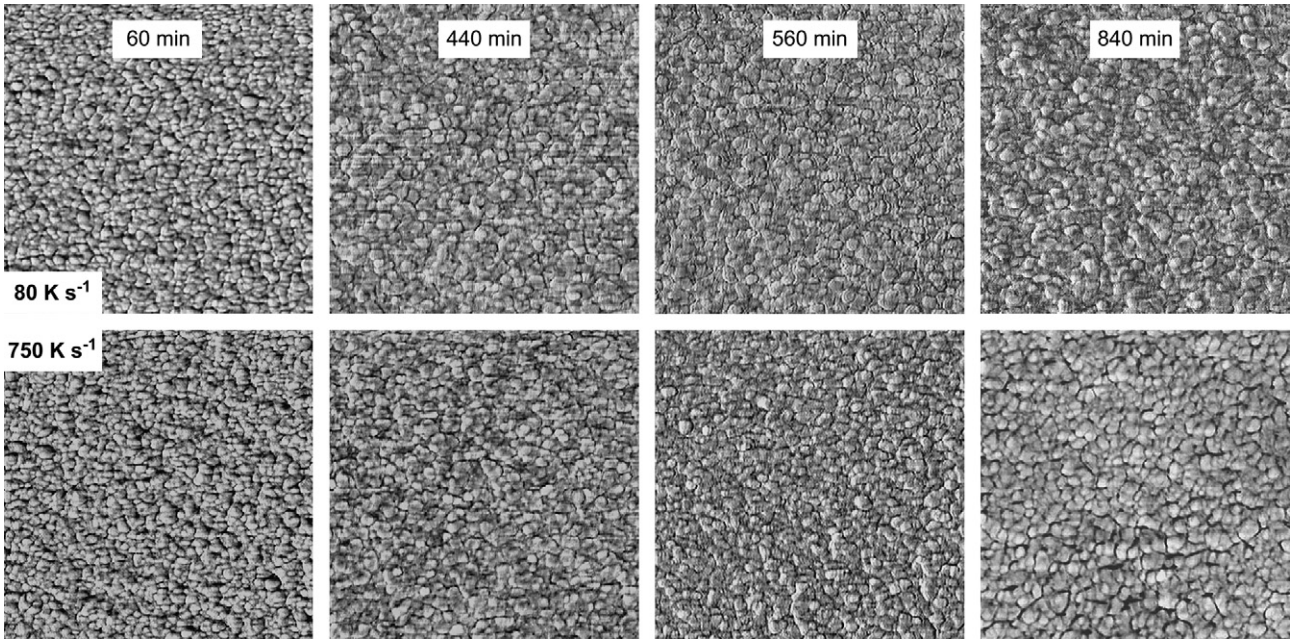

Fig. 2. AFM images of iPP, melt-crystallized at 80 K s^{-1} (top) and 750 K s^{-1} (bottom) cooling rate, taken after isothermal annealing for 60, 440, 560, and 840 min (from left to right) at a temperature of 393 K. The image size is 1 μm × 1 μm.

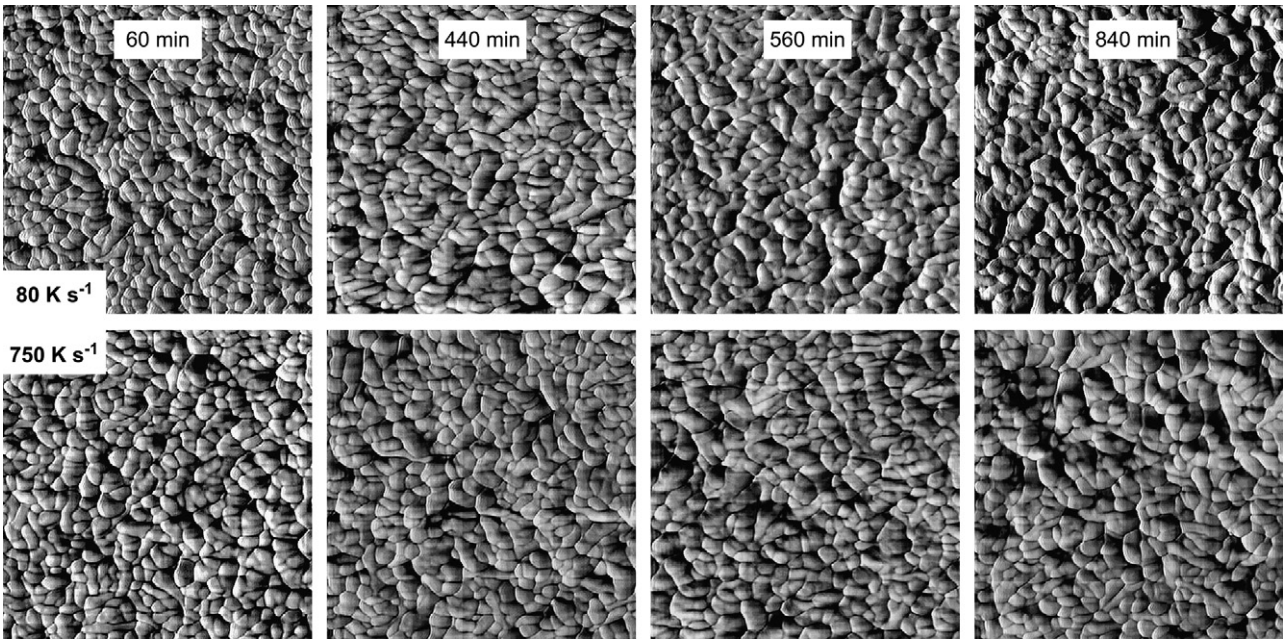

Fig. 3. AFM images of iPP, melt-crystallized at 80 K s^{-1} (top) and 750 K s^{-1} (bottom) cooling rate, taken after isothermal annealing for 60, 440, 560, and 840 min (from left to right) at a temperature of 433 K. The image size is 1 μm × 1 μm.

nodule size during isothermal annealing. The data obtained on the samples which were cooled at 80 K s^{-1} (open symbols) and 750 K s^{-1} (filled symbols) fit a single curve.

3.2. Analysis of isothermal annealing by TMDSC

Fig. 6 shows the apparent specific heat capacity of iPP as a function of the time of isothermal annealing at 393 and 433 K. The thick and thin lines were observed for the samples which initially were melt-crystallized at a rate of 80 K s^{-1} and 750 K s^{-1}, respectively. The samples were heated to the temperature of annealing at a rate of 10 K min^{-1}. The heating scans reveal for both samples, as expected and discussed in the preceding study [5], the mesomorph-to-monoclinic phase transition at about 340 K. The apparent specific heat capacity decreases during annealing as a function time due to irreversible reorganization of the structure, to approach a final constant value after about 500 min. The data obtained on the

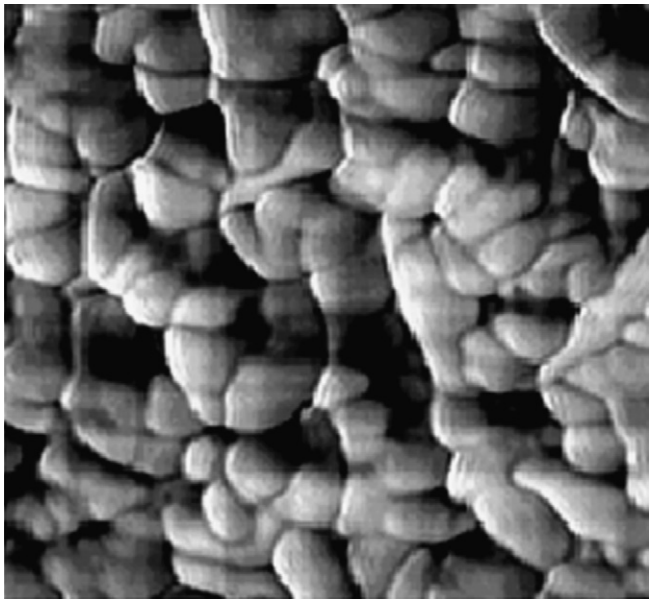

Fig. 4. Enlargement (soft zoom) of an AFM image of iPP, melt-crystallized at 750 K s^{-1}, taken after annealing at 433 K for 840 min. The image size is 500 nm × 500 nm.

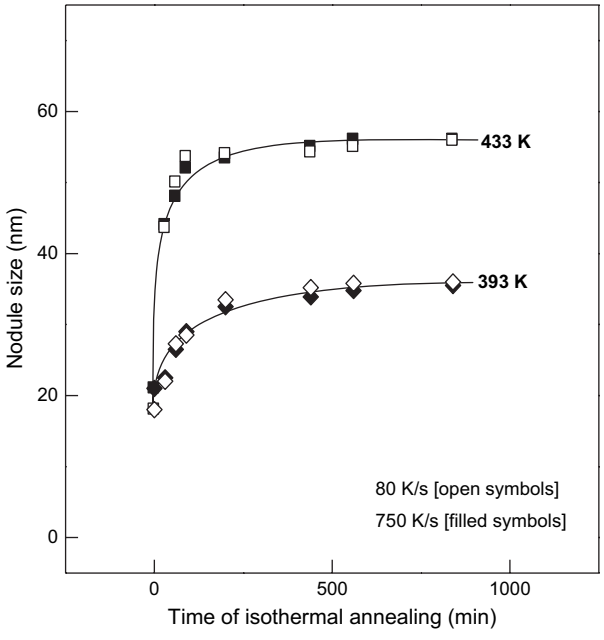

Fig. 5. Size of nodules as a function of the time of isothermal annealing at 433 K (top data, squares) and 393 K (bottom data, diamonds), for iPP samples which initially were melt-crystallized at 80 K s^{-1} (open symbols) and 750 K s^{-1} (filled symbols).

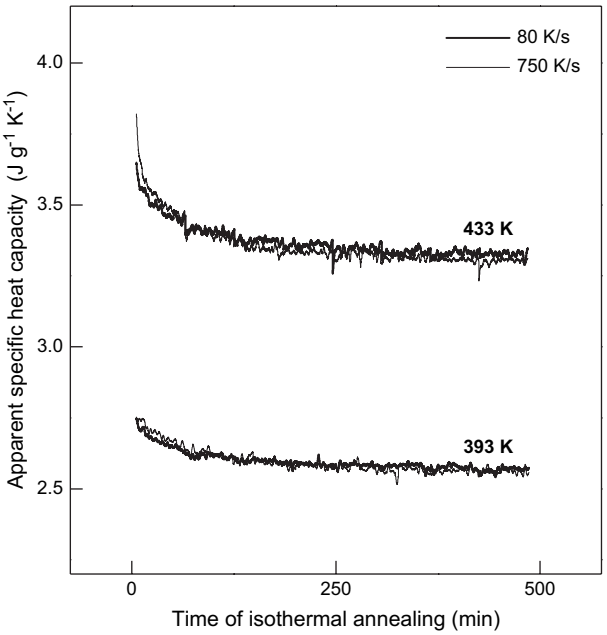

Fig. 6. Apparent specific heat capacity of iPP as a function of the time of isothermal annealing at 433 and 393 K, after initial primary melt-crystallization at 80 K s^{-1} (thick lines) and 750 K s^{-1} (thin lines), and subsequent heating from ambient temperature to the annealing temperature at 10 K min^{-1}.

two samples of different history of initial melt-crystallization are indifferent, similar as in the case of analysis of the nodule size, shown in Fig. 5.

Data recording started after an initial, internal calibration for a period of three modulation cycles, requested by the instruments software and non-controllable by the operator. Thus, first data were available after 6 min of isothermal annealing. Since the apparent specific heat capacity decreases continuously with increasing time of annealing, we assume that the initial values between 0 and 6 min are even larger than the first recorded data. Comparison of the data sets obtained on annealing at 393 and 433 K suggests that the amount of irreversible reorganization of the structure is larger at high temperature since the relative decrease of the apparent specific heat capacity is more distinct at this temperature.

The final apparent specific heat capacity after completed irreversible reorganization is larger after annealing at 433 K, if compared with the final value obtained after annealing at 393 K. The reason is two-fold. The vibrational heat capacity contribution to the apparent specific heat capacity increases with temperature, as it is documented in the ATHAS data base [34]. Furthermore, the final value of the apparent specific heat capacity is affected by reversible crystallization and melting [15,16]. Previous studies revealed that the amount of reversible crystallization and melting during temperature modulation, at a given constant temperature, is proportional to the amount of preceding irreversible crystallization, melting, or reorganization at identical temperature [35]. Since the amount of irreversible change of structure is larger at 433 K, as is concluded from the magnitude of the prior decrease of the apparent specific heat capacity during annealing, the degree of reversible crystallization and melting is also larger.

3.3. Final discussion and conclusions

The present study is the extension of a previous work about the phase structure of iPP after rapid non-isothermal crystallization of the melt, at rates of cooling, which are relevant during conventional processing. Melt-crystallization at a rate faster than about 10^1 K s^{-1} results in the formation of non-lamellar nodular and mesomorphic domains with a size of about 20 nm. These mesomorphic domains are surrounded by amorphous structure, convert to monoclinic structure at about 340 K and change size and habit as function of temperature. The temperature dependence of the crystal geometry was systematically investigated for a larger set of samples which initially were melt-crystallized at rates between 10^1 K $s^{-1}$and 10^3 K s^{-1}. Morphological data were taken as function of temperature after a constant time of isothermal reorganization of 60 min. The effect of time on the evolution of the size and habit of nodules is now further analyzed in the present study for two selected specimens which initially were melt-crystallized at 80 K s^{-1} and 750 K s^{-1}. The reduction of the number of samples, if compared to the previous study, seems justified since the exact condition of initial melt-crystallization, within the analyzed range of cooling rates, on the nodule structure at ambient temperature and on the morphological changes observed at elevated temperature, is negligible. Major changes of the nodule size and geometry were observed at temperatures above about 400 K. The nodule size increased from about 20 nm at ambient temperature to about 23 nm at 403 K, and then further to almost 50 nm at 433 K. The temperature dependence of the nodule size led to the selection of 393 and 433 K for analysis of the evolution of the structure as function of time, since we consider these temperatures as lower and upper boundary for major morphological changes.

Fig. 5 shows a primary result of the present study for the first time the size of nodular crystals of iPP as a function of the time of annealing at 393 and 433 K. The data confirm insensitivity of the time evolution of the nodule size on the exact condition of primary melt-crystallization. In other words, nodules formed at different rates of cooling are similar in their stability. The approach of the annealing temperature does not result in a major change of the initial morphology. Morphological changes are only detected if the temperature is held constant for a certain period of time. The largest changes of the nodule morphology are observed in the initial stage of the annealing process. The fast reorganization of structure is followed by a considerably slower process, which leads only to a minor additional increase of the crystal dimensions. Despite the general time dependence of the isothermal reorganization process of semi-crystalline polymers, containing lamellar crystals, is well-known [36], we did not expect a priori a qualitatively similar time dependence of the isothermal annealing of the non-lamellar crystals of the present study, because of the different thermodynamic stability [37].

Our model of structure reorganization includes, based on experimental data, initial existence of crystals of low thermodynamic stability/melting temperature. These relatively

unstable crystals melt on heating and recrystallize subsequently at the annealing temperature at existing surfaces, i.e., at surfaces of crystals, which still exist at the temperature of annealing. The liquid-crystal transformation accounts for the initial strong increase in the crystal dimensions in the first few minutes of the isothermal annealing procedure. The large number of domains/crystals, produced on initial melt-crystallization at about 300 K, leads to spatial restrictions and limits the lateral growth of crystals. Therefore, a minor but distinct change of the aspect ratio of crystals is observed, as is documented with the non-isotropic geometry of nodules after annealing at 433 K (Fig. 3). Since the number of crystals, melted on prior heating, increases with temperature, the initial increase of the crystal size and change of the crystal shape is more distinct on annealing at 433 K.

The process of fast re-crystallization of liquid is followed by minor and slow continuation of crystal growth. Unfortunately we are not able to identify growth in a preferred crystallographic direction. Most striking on long-term annealing is the observed aggregation of crystals. The aggregation of crystals can be explained by their increased mobility, due to the lowered viscosity of the surrounding amorphous structure at elevated temperature. This process may even include rotation of crystals or positioning of specific crystal faces, for reason of maximum decrease in surface energy, when getting in contact with a neighbored crystal.

The second major intention of the present work is to compare direct morphological observation of the isothermal annealing process with indirect calorimetric analysis. The kinetics of isothermal annealing can conveniently be monitored by TMDSC, by following the decrease of the heat-flow rate amplitude on temperature modulation with an amplitude, which is small enough to allow the approach of an arrested metastable structural equilibrium. TMDSC has successfully been applied for analysis of the annealing kinetics of numerous semi-crystalline polymers. The decrease of the amplitude of the modulated heat-flow rate, which is proportional to the apparent specific heat capacity during isothermal annealing, in many cases, is mathematically described by superposition of several, up to three exponential functions with different time constants [23,38], or by using a stretched exponential, Kohlrausch–Williams–Watt type function [27,39]. By measurement of the temperature dependence of kinetic constants, even activation energies were extracted, which, in part, are similar in magnitude to that of the α-relaxation at the crystal–amorphous interface, usually analyzed by dynamic mechanical analysis [38,39]. Regardless the considerable advances in application of TMDSC for analysis of thermodynamic properties and phase transitions in polymers in recent years [22], there often remains uncertainty in the interpretation of results since a conversion of the energy-based apparent specific heat capacity, given in $J\,g^{-1}\,K^{-1}$, or of the heat of transition, given in $J\,g^{-1}$, to direct structural information is speculative. As far as we are aware of, there is no report to date which compared calorimetric with microscopic data, as a further attempt for an in-depth interpretation of reorganization of semi-crystalline polymers towards a new metastable equilibrium.

First of all we see remarkable agreement in the time dependence of the increase of the nodule size (Fig. 5) and decrease of the apparent specific heat capacity (Fig. 6). In Fig. 7, the data of Figs. 5 and 6 were re-plotted such that a direct comparison is possible. The nodule-size data were multiplied by (−1), and subsequently shifted vertically for easy recognition. Note furthermore, also for the sake of clarity, that in Fig. 7 no distinction is made between the samples, which initially were crystallized at different rates. The decrease of the apparent specific heat capacity goes parallel with the observed change of the nodule size. This holds for the initial part as well as for the later stage of the annealing process. Even the specific differences due to annealing at different temperatures are recovered. The initial decrease of the apparent specific heat capacity is considerably larger on annealing at 433 K, compared to the annealing experiment at 393 K. The apparent specific heat capacity decreases within the analyzed range of time between 6 and 485 min by about $0.4\,J\,g^{-1}\,K^{-1}$ [$\approx$(3.70–3.32) $J\,g^{-1}\,K^{-1}$] during annealing at 433 K, and by about $0.2\,J\,g^{-1}\,K^{-1}$ [$\approx$(2.75–2.56) $J\,g^{-1}\,K^{-1}$] during annealing at 393 K. The different final values of the apparent specific heat capacity of 3.32 and $2.56\,J\,g^{-1}\,K^{-1}$ after annealing at 433 and 393 K, respectively, are due to (a) the temperature dependence of the vibrational specific heat capacity [34], and (b) different amounts of reversible melting [15]. The major decrease of the apparent specific heat capacity is within the first 200 min, then the curves go almost parallel. In a previous TMDSC study on the annealing process in polyethylene, the modulated heat-flow rate was analyzed in the time domain which led to the conclusion that at least in the initial part of the annealing process the increased apparent heat capacity is mainly due to exothermic heat flow [23]. This is confirmed by close inspection of heat-flow rate in a standard DSC experiment, when switching from the heating segment to the

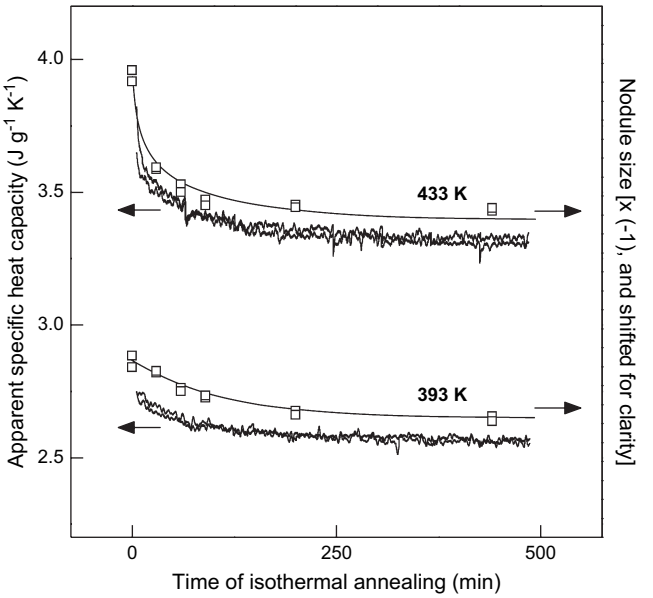

Fig. 7. Apparent specific heat capacity (left axis), and nodule size, re-calculated as described in the text, (right axis) as a function of the time of isothermal annealing at 433 and 393 K.

isothermal segment [40]. With the AFM observations of the present study we can now unambiguously derive the conclusion, that the exothermic heat flow is connected with an increase in the crystal size. Annealing at 393 K produces less heat of crystallization than annealing at 433 K, as can directly be concluded from the different offsets of the apparent specific heat capacity of about 0.2 and 0.4 $J\,g^{-1}\,K^{-1}$, respectively, above the final value after extrapolated infinity annealing time. This is in excellent agreement with the much reduced increase of the crystal size after annealing at 393 K.

The continued decrease in the apparent specific heat capacity after about 200 min is difficult to link to a specific reorganization process. We do not believe, or have any evidence, that this decrease is connected to the process of aggregation, which is the major microscopic observation, at least on annealing at 433 K. Furthermore, the decrease of the apparent specific heat capacity is also obtained on long-term annealing of laterally extended lamellae, which do not aggregate as the nodules of the present study. The continued minor decrease of the apparent heat capacity may be caused by continued secondary crystallization, i.e., by continuation of the same process which is responsible for the initial strong decrease, or by crystal perfection which is not accessible by microscopy.

Recent comparison of the annealing process of iPP, which contained either lamellar or nodular crystals, revealed that the kinetics is almost indifferent. The data of the present study confirm that annealing of nodular crystals is controlled by identical mechanisms from calorimetric point of view.

Acknowledgments

This research was partially supported by funding from the ministry of culture of Saxony-Anhalt (Germany), and by a STSM grant within the EU COST-P12 program for one of the authors (Q.Z.).

References

[1] Piccarolo S. J Macromol Sci Phys 1992;B31:501–11.
[2] Piccarolo S, Alessi S, Brucato V, Titomanlio G. In: Dosiere M, editor. Crystallization of polymers. NATO ASI series. Series: C mathematical and physical sciences. Kluwer; 1993. p. 475–80.
[3] Brucato V, La Carubba V, Piccarolo S, Titomanlio G. Int Polym Proc 1999;14:1–7.
[4] Brucato V, Piccarolo S, La Carubba V. Chem Eng Sci 2002;57:4129–43.
[5] Zia Q, Androsch R, Radusch HJ, Piccarolo S. Polymer 2006;47:8163–72.
[6] De Santis F, Adamovsky S, Titomanlio G, Schick C. Macromolecules 2006;39:2562–7.
[7] Fichera A, Zannetti R. Die Makromol Chem 1975;176:1885–92.
[8] Zannetti R, Celotti G, Fichera A, Francesconi R. Die Makromol Chem 1969;128:137–42.
[9] Caldas V, Brown GR, Nohr RS, MacDonald JG, Raboin LE. Polymer 1994;35:899–907.
[10] Nishida K, Konishi T, Kanaya T, Kaji K. Polym Commun 2004;45:1433–7.
[11] Ogawa T, Miyaji H, Asai K. J Phys Soc Jpn 1985;54:366–3670.
[12] Wang ZG, Hsaio BS, Srinivas S, Brown GM, Tsou AH, Cheng SZD, et al. Polymer 2001;42:7561–6.
[13] Grubb DT, Yoon DY. Polym Commun 1986;27:84–8.
[14] Hsu CC, Geil PH, Miyaji H, Asai K. J Polym Sci Polym Phys 1986;24:2379–401.
[15] Androsch R, Wunderlich B. Macromolecules 2001;34:5950–60.
[16] Androsch R, Wunderlich B. Macromolecules 2001;34:8384–7.
[17] Wunderlich B. In: Crystal nucleation, growth, annealing. Macromolecular physics, vol. 2. New York: Academic Press; 1976.
[18] Wunderlich B. In: Crystal melting. Macromolecular physics, vol. 3. New York: Academic Press; 1980.
[19] Reading M, Hahn BK, Crowe BS. Method and apparatus for modulated differential analysis. U.S. Patent 5,224,775, July 6, 1993.
[20] Gill PS, Sauerbrunn SR, Reading M. J Therm Anal 1993;40:931–9.
[21] Boller A, Jin Y, Wunderlich B. J Therm Anal 1994;42:307–29.
[22] Androsch R, Wunderlich B. In: Matyjaszewski K, Gnanou Y, Leibler L, editors. Scanning calorimetry. Macromolecular engineering: precise synthesis, materials properties, applications, vol. 3. Wiley-VCH; 2007.
[23] Androsch R, Wunderlich B. Macromolecules 1999;32:7238–47.
[24] Androsch R, Wunderlich B. Macromolecules 1999;30:9076–89.
[25] Androsch R. J Therm Anal Calorim 2004;77:1037–43.
[26] Okazaki I, Wunderlich B. Macromolecules 1997;30:1758–64.
[27] Schick C, Merzlyakov M, Wunderlich B. Polym Bull 1998;40:297–303.
[28] Pyda M, Wunderlich B. J Polym Sci Polym Phys 2000;38:622–31.
[29] Androsch R, Wunderlich B, Radusch HJ. J Therm Anal Calorim 2005;79:615–22.
[30] Private communication, Basell Bayreuth Chemie GmbH 2001.
[31] Wunderlich B. Thermal analysis of polymeric materials. Berlin: Springer; 2005.
[32] Androsch R, Moon I, Kreitmeier S, Wunderlich B. Thermochim Acta 2000;357–358:267–78.
[33] Androsch R, Wunderlich B. Thermochim Acta 1999;333:27–32.
[34] Wunderlich B. Pure Appl Chem 1995;67:1019–26.
[35] Androsch R, Wunderlich B. J Polym Sci Polym Phys 2003;41:2039–51.
[36] Fischer EW. Kolloid Z Z Polym 1969;231:458–503.
[37] Crist B. Macromolecules 2006;39:1971–80.
[38] Höhne GWH, Kurelec L, Rastogi S, Lemstra PJ. Thermochim Acta 2003;396:97–108.
[39] Huang Z, Marand H, Cheung WY, Guest M. Macromolecules 2004;37:9922–32.
[40] Androsch R. Unpublished data 2007.